Turbulence Transition in Pipe Flow

Bruno Eckhardt,[1] Tobias M. Schneider,[1]
Bjorn Hof,[2] and Jerry Westerweel[3]

[1]Fachbereich Physik, Philipps-Universität Marburg, D-35032 Marburg, Germany;
email: bruno.eckhardt@physik.uni-marburg.de

[2]Department of Physics and Astronomy, University of Manchester, Manchester,
M13 9PL, United Kingdom

[3]Laboratory for Aero and Hydrodynamics, Delft University of Technology,
2628 CA Delft, The Netherlands

Annu. Rev. Fluid Mech. 2007. 39:447–68

The *Annual Review of Fluid Mechanics* is online
at fluid.annualreviews.org

This article's doi:
10.1146/annurev.fluid.39.050905.110308

0066-4189/07/0115-0447$20.00

Key Words

shear flows, coherent structures, nonlinear dynamics, chaotic saddle

Abstract

Pipe flow is a prominent example among the shear flows that undergo transition to turbulence without mediation by a linear instability of the laminar profile. Experiments on pipe flow, as well as plane Couette and plane Poiseuille flow, show that triggering turbulence depends sensitively on initial conditions, that between the laminar and the turbulent states there exists no intermediate state with simple spatial or temporal characteristics, and that turbulence is not persistent, i.e., it can decay again, if the observation time is long enough. All these features can consistently be explained on the assumption that the turbulent state corresponds to a chaotic saddle in state space. The goal of this review is to explain this concept, summarize the numerical and experimental evidence for pipe flow, and outline the consequences for related flows.

1. INTRODUCTION

Transition to turbulence in pipe flow has puzzled scientists since the studies of Gotthilf Heinrich Ludwig Hagen (Hagen 1839, 1854), Jean Louis Marie Poiseuille (Poiseuille 1840), and, most prominently, Osborne Reynolds in 1883 (Reynolds 1883). Under favorable conditions, when the water in the supply tank had settled and the inflow was controlled with suitable funnels, Reynolds was able to maintain laminar flow until the mean flow speed was equivalent to $Re = 12000$, when expressed in the dimensionless combination of mean flow speed $\overline{u}$, pipe diameter d, and viscosity ν that now carries Reynolds's name: $Re = \overline{u}d/\nu$. On the other hand, with sufficiently strong perturbations he was able to trigger a transition near Reynolds numbers of about 2000. A more precise value above which transition to turbulence can be triggered is difficult to identify, with quoted values ranging between 1760 and 2300 (Kerswell 2005).

Pipe flow differs from many other flow situations in that the laminar profile is linearly stable for all Reynolds numbers: All sufficiently small perturbations will decay [see, e.g., Salwen et al. (1980) and, in particular, Meseguer & Trefethen (2003), who analyzed the problem up to $Re = 10^7$]. Thus, to trigger transition, two thresholds have to be crossed: The flow has to be sufficiently fast and a perturbation has to be strong enough. Observing a section of the pipe fixed in the lab frame gives the familiar intermittent switching between laminar and turbulent regions: A sufficiently large perturbation triggers turbulence, which is then swept past the observation region, and the flow becomes laminar until another sufficiently strong perturbation again induces turbulence. This behavior was demonstrated using Reynolds's original experiment by Homsy et al. (2004). **Movies of the experiment and some flow visualizations** may be found via the Supplemental Material link from the Annual Reviews home page at **http://www.annualreviews.org**. Further experiments by Hof et al. (2003) show that as the Reynolds number increases the critical threshold decreases so that at sufficiently high Reynolds numbers the unavoidable residual fluctuations always suffice to trigger turbulent flow. Exactly how the threshold depends on the Reynolds number is an intriguing question that is discussed in some detail in Section 2, with a refinement in Section 5.

A second feature of transition to turbulence in pipe flow is that between the laminar and turbulent state there exists no state with simple spatial or temporal structures, unlike the rolls in Rayleigh-Bénard or the Taylor vortices in Taylor-Couette flows, for example. Moreover, numerical simulations by Brosa (1989) and Faisst & Eckhardt (2004), and also the experimental results of Darbyshire & Mullin (1995), Hof (2004), Mullin & Peixinho (2006), and Peixinho & Mullin (2006), show that even if one establishes a state with all features of turbulent dynamics, this state can still decay without any clear precursors: Although it is relatively easy to conclude that the further dynamics will be a relaxation toward the laminar profile, for instance, because the energy in the radial component of velocity drops below a certain value, there is no indicator for the imminent decay. This property of the flow is considered in Section 3.

The understanding of the properties of transition in pipe flow that has emerged in the past few years rests on the application of the appropriate model in dynamical system theory and systematically designed numerical and laboratory experiments.

The background for these studies is the abstraction to consider the system in its state space (Lanford 1982). Physically, it is the space of all velocity fields, either prepared as initial conditions or obtained in the time evolution of the flow. Mathematically, it is spanned by all divergence-free flow fields that satisfy the appropriate boundary conditions, represented, for instance, by the coefficients of an expansion of velocity fields in a complete basis of orthonormal basis functions. The state space contains the laminar profile and the turbulent flow fields. Coherent structures such as vortices, streaks, hairpins (Panton 2001, Robinson 1991), or traveling waves (Hof, van Doorne et al. 2004) occupy different parts of the state space. The state space should provide a complete description of the dynamics, in that at any point in this space the Navier-Stokes equations together with boundary conditions uniquely determine the evolution. The time evolution of a flow then traces out a continuous trajectory in this state space. We assume that ideas developed in the context of finite-dimensional dynamical systems can be applied to this infinite-dimensional situation (see Doering & Gibbon 1995 for a discussion of the subtleties involved).

In state space, there is one region dominated by the laminar flow. The time-independent parabolic profile is a fixed point in this space. The parabolic profile is linearly stable and, hence, all points in its neighborhood evolve toward the fixed point; these states form the basin of attraction of the laminar flow. The turbulent dynamics take place in other parts of the state space. If turbulence was an attractor (Guckenheimer 1986, Lanford 1982), then it, too, would have a basin of attraction so that all initial conditions close to it would be attracted to the turbulent dynamics. The spatially and temporally fluctuating dynamics of the turbulent regions suggests that there are chaotic elements, such as horseshoes, just as in a regular attractor (Guckenheimer & Holmes 1983). However, the possibility of decay indicates that the basin is not compact nor space filling; there must be connections to the laminar profile. In dynamical systems such structures are known as chaotic saddles or strange saddles: With chaotic attractors they share positive Lyapunov exponents for the motion close to the saddle, but they are not persistent and have a constant probability of decay.

The idea of transient chaos is familiar from the motion of interacting point vortices (Aref 1983, Aref et al. 1988, Eckhardt & Aref 1988). Several vortices carrying vorticity of equal sign spin around each other, and if their number exceeds three the motion is most likely chaotic. Pairs of equal but opposite vorticity can escape to infinity along straight lines. One can then set up a scattering experiment by aiming two vortex pairs against each other. Upon collision they can exchange partners, and if the net vorticity in each pair does not vanish, they move in circles until the next collision. If the original partners do not regroup, the circular motion continues until the next collision. Except for meticulously chosen initial conditions this motion ends and the pairs separate again. The time at which this happens depends sensitively on initial conditions and slight variations can lead to widely differing trapping times (Aref et al. 1988, Eckhardt & Aref 1988). However, among all the chaotic trajectories there do exist some with fairly regular dynamics: periodic solutions embedded in a sea of chaos. They can be used to describe segments of trajectories and can be pieced together as building blocks for more complicated motion. They have at least one unstable direction and several stable ones, so that the motion in their vicinity is akin

to that near a saddle. In a chaotic saddle the stable and unstable directions tangle to form the principle element of chaotic motion, a Smale horseshoe (Guckenheimer & Holmes 1983).

Another analogy to help one visualize the meaning of a chaotic saddle is that of a particle in a box with curved walls (Ott 1993). The particle dynamics is such that the particle moves along straight lines until it hits a wall where it is elastically reflected. With the exception of a spherical, ellipsoidal, or rectangular shape, nearly any boundary will produce chaotic particle dynamics. The fact that this model is energy conserving whereas a hydrodynamic flow is dissipative should not be of concern: If the dynamics is expanded to include friction on the particle and a motor that keeps the particle in motion, one arrives at a dissipative analog with the same key features. To obtain a chaotic saddle, introduce a hole into the wall through which the particle can escape. Until the particle hits the hole it will bounce around chaotically, and the dynamics will have a positive Lyapunov exponent λ. Because of the positive Lyapunov exponent, correlations in trajectories will disappear quickly (on a timescale of the order of $1/\lambda$), and the probability of hitting the escape hole remains nearly the same: Whenever the particle hits the wall it escapes with a probability equal to the area of the hole divided by the total surface area.

There are three implications of a strange saddle that can be observed in pipe and other shear flows: (*a*) the (transient) turbulent dynamics has a positive Lyapunov exponent, (*b*) the distribution of lifetimes becomes exponential for long times, and (*c*) the hyperbolic elements in the turbulent dynamics show up as transient patterns in the turbulent flow. Of these, a Lyapunov exponent has only been determined in numerical simulations (Faisst & Eckhardt 2004) as it requires a comparison of the time evolution of two states starting from nearby initial conditions–a feat not yet achieved in experimental studies. For the latter two implications, there are both experimental and numerical results. Lifetime statistics were obtained by repeating experiments with long observation times for different initial conditions, and certain coherent elements that may serve as the invariant structures around which the chaos develops were identified. The evidence for the lifetimes is discussed in Section 3, and the relation between chaotic saddles and coherent structures is the subject of Section 4.

The state space picture with separate domains for the laminar and turbulent dynamics raises a question regarding the border between the two. The precise nature of this border is complicated, especially in view of the transient nature of turbulence. But it is clear that, depending on which side of the border a perturbation starts out, it will either swing up to the turbulent region or decay to the laminar profile. This can be exploited in order to find the border and to trace the dynamics along it. The precise nature of this border as well as observations regarding the dynamics in this region are discussed in Section 5.

In the subsequent sections we summarize the experimental and numerical evidence for this transition scenario and outline a few consequences. However, there is one element of transition to turbulence in pipe flow that is not addressed: For the intermediate Reynolds numbers considered here a localized perturbation will induce turbulence in localized sections of the pipe only (see Wygnanski & Champagne 1973 and Wygnanski et al. 1975 for seminal observations and studies). These turbulent

puffs and slugs typically extend about 30 diameters along the axis and move downstream with little change in axial extent. It is desirable to explain this localization of the turbulence as well, but this is not yet possible. We expect that this problem falls into the class of "patterned turbulence phenomena" that includes the turbulent patches in shear flows (Gad-el-Hak & Hussain 1986, Schumacher & Eckhardt 2001), or the striped turbulence in Taylor-Couette (Prigent et al. 2002) and plane Couette flow (Barkley & Tuckerman 2005, Bottin & Chate 1998, Bottin et al. 1998). As in the modeling attempt of Prigent et al. (2002), one may build on the assumption that on top of the short-time, short length-scale turbulent interior dynamics, there is a long wavelength modulation that is responsible for the structuring. The interior and envelope dynamics may be linked at the front and trailing edges because of the similar structures that can be detected there, but we do not yet know enough about their relation. The separation in length scales (the typical structures to be discussed below are only a few diameters long) and numerical evidence from turbulent spots, which sometimes decay from within, and not by retreating boundaries (Schumacher & Eckhardt 2001), suggest that one should be able to separate the dynamics of the turbulent boundaries from the dynamics of the chaotic elements discussed below.

Various aspects of transition in shear flows in the absence of linear instability were recently reviewed. Grossmann (2000) summarized the physics of non-normal amplification and its consequences for threshold behavior. Kerswell (2005) surveyed experimental and theoretical work culminating in the detection of the traveling waves that we consider in Section 4. The proceedings of a 2004 conference in Bristol (Mullin & Kerswell 2005) contain a useful collection of articles on several current approaches to the problem. This review focuses on pipe flow, and describes the methods used to analyze transition and the turbulent dynamics. We hope this will be helpful for gaining insight in other shear flows for which pipe flow can serve as a model: In several respects, transition to turbulence in these shear flows differs from the more traditional ones in Rayleigh-Bénard or Taylor-Couette and belongs to a class of its own.

In Section 2 we review the experiments on the transition, followed by a study of the lifetimes in Section 3. A survey of coherent structures is presented in Section 4, and an analysis of the border between the laminar and turbulent regions is in Section 5. We conclude with a summary on pipe flow in Section 6 and an outlook to related flows and open issues in Section 7.

2. TRANSITION EXPERIMENTS

Because the laminar profile is linearly stable for all Reynolds numbers, a finite stimulus is needed to trigger the transition. In typical experiments this is achieved by injecting or removing liquid from the pipe.

In a stimulating set of experiments Darbyshire & Mullin (1995) tried to identify the critical amplitude for perturbations that trigger transition. Their findings are revealing. Repeating the experiment with initial conditions that were identical within experimental resolution gave widely differing results: Sometimes transition was induced, and sometimes not. The observation of transition for one set of

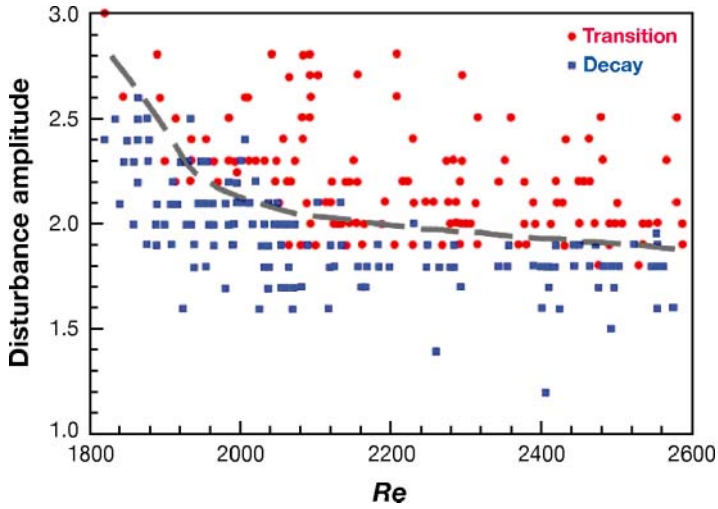

Figure 1

Transition experiments by Darbyshire & Mullin (1995). Disturbances were introduced at a distance 70 diameters downstream of the inlet, and their status was probed at another 120 diameters downstream, delayed with the mean advection time. Depending on whether the perturbation was still present or not, a point was marked "transition" or "decay." The amplitude of the perturbations is proportional to the injected fluid volume. For more details, see Darbyshire & Mullin (1995). Redrawn after Darbyshire & Mullin (1995).

initial conditions gave no insight regarding the behavior of neighboring conditions: Sometimes they remained turbulent, and sometimes they decayed. **Figure 1**, which summarizes their findings, does not show a clear separation between decaying and turbulent initial conditions.

The sensitivity of transition to initial conditions is best studied in numerical simulations, where within the confines of the numerical representation and algorithms one has perfect control over the initial conditions and can study the evolution of slightly differing initial conditions (Faisst & Eckhardt 2004). Moreover, because of the continuous monitoring of the dynamics one can determine the time when the energy content in the perturbation drops below a level from which it cannot recover, so that one has entered the basin of attraction of the laminar profile. This defines the lifetime. Numerical experiments for pipe flow show a very rapid variation in lifetimes depending on initial condition and Reynolds number (see **Figure 2**). The data of Darbyshire & Mullin (1995) can be obtained from such a lifetime plot by slicing at a prescribed time level T_0: Anything with lifetimes above T_0 qualifies as turbulent, and anything below as decay. In **Figure 2**, the presence of valleys and pinnacles corresponds to the isolated decaying initial conditions surrounded by turbulent ones and vice versa in **Figure 1**.

The small-amplitude region of the graph allows one to quantify the increased sensitivity of the flow to perturbations with increasing Reynolds number. At high Re, lower perturbation amplitudes are needed to trigger turbulence. A linear analysis of perturbations around the laminar profile shows that certain perturbations

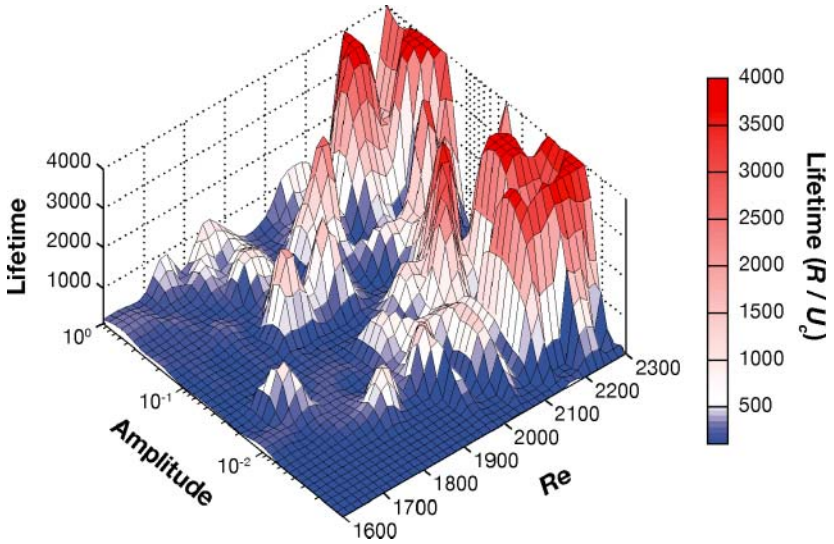

Figure 2

Numerical transition experiments. A flow was prepared with an initial condition consisting of the parabolic profile with center speed u_c and a perturbation with fixed spatial structure but varying amplitude. The flow was evolved until it either decayed or exceeded the maximal integration time.

can give rise to flow fields whose amplitude transiently increases before eventually succumbing to decay (Grossmann 2000; Schmid & Henningson 1999, 1994). The origin of this mechanism lies in the non-normal nature of the linearized equations of motion (Boberg & Brosa 1988, Trefethen et al. 1993) and becomes transparent when the relevant flow structures are studied (Hamilton et al. 1995, Panton 2001): A downstream vortex mixes fluid across the shear direction and thereby sets up streamwise modulations of the streamwise velocity, thus forming the known boundary-layer streaks. Simple estimates, confirmed by more detailed studies, suggest that a vortex of strength O(1/Re) can generate a streak of order O(1), that is a *Re*-fold increase in velocity amplitude (Chapman 2002, Henningson 1996, Waleffe 1995). Experiments reported in Hof et al. (2003), Hof (2004), and Draad et al. (1998) give evidence for a scaling of the critical amplitude like 1/*Re* in the Reynolds number range between 2000 and 20,000.

3. LIFETIME STATISTICS

The strong sensitivity of the lifetimes on initial conditions suggests a limited meaning to individual trajectories for transition studies. Statistical properties like the distribution of lifetimes are a more reliable means for transition studies. The prediction of dynamical systems theory for the lifetimes of a chaotic saddle is that the probability of decay is independent of the time that has elapsed since the turbulent state was created, and that therefore the distribution of lifetimes is an exponential (Kadanoff & Tang 1984).

In the experiments by Darbyshire & Mullin (1995), the state of the system was only analyzed at the end of a fixed-length pipe. By following the perturbation as it moves with the mean flow, one can determine the point where it decays. These observations

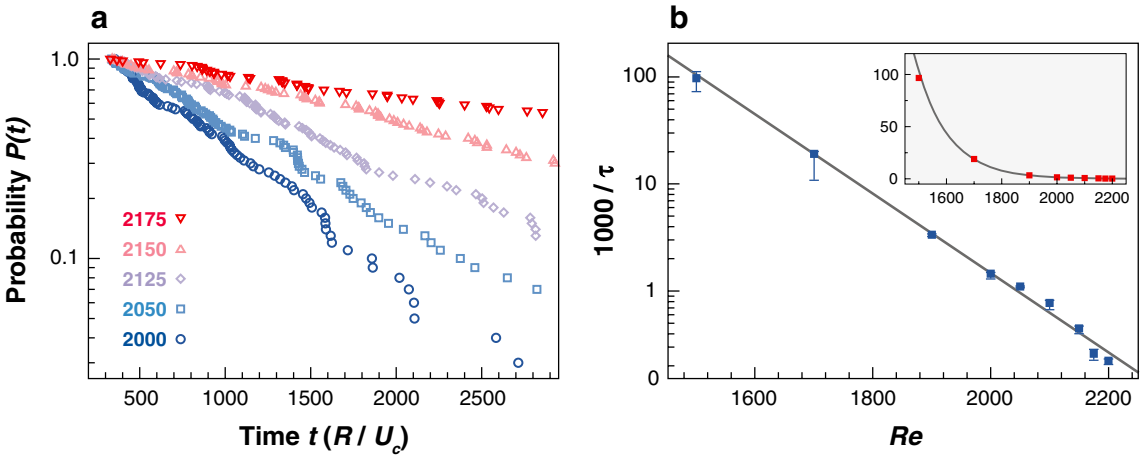

Figure 3

Lifetimes of perturbations in pipe flow. (*a*) The left frame shows the probability $P(t)$ to be turbulent at least for a time t for different Reynolds numbers. (*b*) The right frame shows the rapid increase of the characteristic time of the exponential fit. The straight line in the semilogarithmic plot indicates an exponential increase. The inset demonstrates that a linear variation of the inverse of the characteristic time with Reynolds number does not represent the data.

are applied in the determination of the probability $P(t)$ that the flow remains turbulent for at least a time t. If the turbulent state were permanently sustained, the lifetimes would be infinite, $P(t) = 1$. If the probability of decay in some time interval δt is constant and independent of the time that has elapsed from the start of the experiment, an exponential distribution is obtained, $P(t) \propto \exp(-t/\tau)$. It is characterized by a time τ, equal to the time over which the probability drops by $1/e$. For all data analyses one has to keep in mind that the exponential form is a statement about the long-time behavior, i.e., it is safest to obtain τ from the slope in a semilogarithmic representation.

Numerical experiments give the distribution shown in **Figure 3*a***. For short times there is a nonuniversal part that depends on the type and duration of the stimulus. However, independent of the initial condition, the tail of the distribution for long times becomes exponential. This hallmark of transient strange saddles has also been found, experimentally (Bottin & Chate 1998) and numerically (Eckhardt et al. 2002), in plane Couette flow.

Figure 3*b* shows the variation of the characteristic time τ with Reynolds number. The characteristic time increases rapidly with Re, but there is no theoretical prediction for the functional form of this variation. Low-dimensional systems provide examples with algebraic (Kaneda 1990), exponential (Moehlis et al. 2004), and even superexponential increases (Crutchfield & Kaneko 1988). Following a similar analysis for plane Couette flow by Bottin & Chate (1998), Eckhardt & Faisst (2004) studied the inverse of the characteristic time and found evidence for a divergence of the characteristic time τ(Re) near Re = 2250. This would indicate a transition from a transient

chaotic saddle to a persistent chaotic attractor. In dynamical systems, the reverse—the destruction of a chaotic attractor by some form of boundary crisis—has been studied frequently (Grebogi et al. 1982). Experimental results by Mullin & Peixinho (2006) and Peixinho & Mullin (2006) also show a divergent characteristic time, but at a lower Reynolds number of about 1750. The most recent analyses of experiments in a very long pipe with observation times up to 7500 d/ū and of additional numerical data suggest that the characteristic time does not diverge, but instead increases exponentially with Reynolds number (Hof et al. 2006). Such a behavior implies that at any Reynolds number and in the neighborhood of every turbulent trajectory there will be some trajectories that decay toward the laminar profile. However, the times over which this happens quickly become inaccessibly large. Hof et al. (2006) estimate that for a typical garden hose at $\mathrm{Re} = 2380$ a pipe length of 40,000 km and an observation time of five years are required to observe the decay. Nevertheless, the time for relaminarization can be reduced by targeting the system onto the appropriate trajectories. Clearly, this unexpected observation requires further experimental and numerical analysis, in pipe flow and other shear flows. In particular, the influences of numerical resolution and domain size, or of external and internal perturbations in experiments, need to be explored further. In all cases the main challenge is to obtain good statistics for very long observation times where the theoretical prediction of an exponential lifetime distribution is realized.

To establish the chaotic nature of the transient dynamics in relation to the models mentioned in the Introduction, it is valuable to determine the short-time Lyapunov exponent using, for instance, the method described in Eckhardt & Yao (1993). For Reynolds numbers near $\mathrm{Re} = 2200$, one finds Lyapunov exponents of about $0.07\, u_c/R$, based on laminar center line speed u_c and radius R (Faisst & Eckhardt 2004). After advection downstream by 10 radii, the difference between two initial conditions as measured, for instance, by the maximum of the pointwise difference between the velocity fields, increases by a factor of two. Setting up experiments that are close to within 10% after traveling 100 diameters downstream requires one to control initial conditions to within 10^{-4}! This indicates the chaotic nature of pipe flow. The positive Lyapunov exponent can also be used to rationalize the rapid variations of lifetimes with flow parameters. Suppose that after a time t one state decays, but a neighboring one, which is a distance d_e away, does not. A variation in initial conditions of order $d_e \exp(-\lambda t)$ can suffice to shift the flow that decays into the one that remains turbulent for a much longer time. Whether a turbulent flow will continue to be turbulent beyond this time or whether it will decay can only be predicted if the full flow field can be described with such accuracy! This explains why the decay of a specific initial condition is unpredictable, and why there are significant variations in lifetimes between different initial perturbations or different Reynolds numbers.

4. CHAOTIC SADDLES AND COHERENT STATES

Embedded in all chaotic motions are simpler, more regular time evolutions. For instance, for the vortex pairs mentioned in the Introduction one can find uniformly propagating states with pairs regularly circling around each other (Aref et al. 1988).

Similarly, for the chaotic container in the previous section there are often trajectories that bounce back and forth along a diameter. Typically, neither of these motions are stable, but they are significant, as they can be used to establish chaos by proving the presence of chaotic horseshoes, and they can dominate the visual appearance of the dynamics.

For the shear flows we consider here, the first example of a more regular solution to the equations of motion embedded in the turbulent dynamics was found in plane Couette flow by Nagata (1990), Clever & Busse (1992, 1997), and Waleffe (2003) (see Cherhabili & Ehrenstein 1997 for a different class of solutions). They were called tertiary structures to distinguish them from the primary structures that appear in bifurcations from the linear profile and secondary ones that appear in subsequent bifurcations of primary ones. Quartenary structures are in turn derived from linear instabilities of tertiary structures. Plane Couette flow has an up-down symmetry in the mean profile so that one can find stationary states. If the up-down symmetry is broken in the three-dimensional (3D) states, the stationary solutions turn into traveling waves. For plane Poiseuille flow, these states appear as traveling waves from the beginning (Ehrenstein & Koch 1991, Waleffe 2003). Remarkably, all these states are dominated by large-scale features, prominent vortices, and streaks, and they qualify as coherent structures.

4.1. Coherent States in Pipe Flow

Finding such coherent states in pipe flow is made difficult by the absence of a bifurcation that could be used as a starting point, and a Newton search from an arbitrary initial condition will typically not converge. However, as in other cases, an embedding in a family of flows can provide the desired starting point. For plane Couette flow an embedding in a Rayleigh-Bénard situation with differential heating across the plates (Clever & Busse 1992, 1997; Nagata 1990) or a Taylor-Couette flow with a narrow gap (Faisst & Eckhardt 2000) shows that some 3D stationary states can be continued over to the original plane Couette flow. These states are dominated by downstream vortices wiggling in the spanwise direction. They are intriguing because they are similar to the ones that give the strongest non-normal amplification (Schmid & Henningson 1999, 1994; Zikanov 1996).

For pipe flow there is no natural embedding in a larger family of flows with instabilities. But by adding body forces that drive downstream vortices one can set up an artifical system with the desired properties. The detailed choice of body force is not critical: Wedin & Kerswell (2004) first solved the linear system and used the least-damped streamwise rolls as a starting point, but the intuitive choice of Faisst & Eckhardt (2003) leads to the same coherent states. The search proceeds in two steps: Pick a Reynolds number and a body force sufficiently large such that the vortices undergo a bifurcation in which 3D states are created. In particular, if the initial states are translationally invariant, this symmetry must be broken. Next, try to follow the 3D states over to pipe flow without body force.

Motivated by the arrangements of vortices in plane Couette flow and the radial shear flow, Faisst & Eckhardt (2003) started with flows containing several pairs of

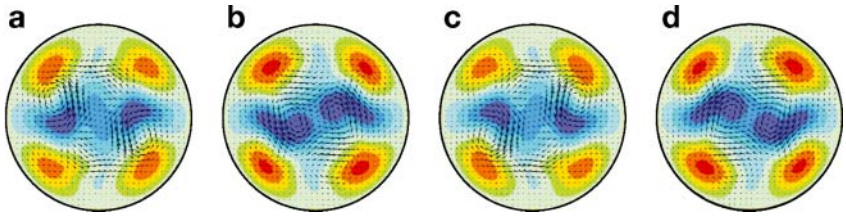

Figure 4

Cross sections of a traveling wave at different positions along the wave. The frames are at times 0, 1/8, 2/8, and 3/8 of a period and at a fixed position along the axis. The velocity components in the plane are indicated by arrows. For the axial component the difference to a parabolic profile with the same mean speed is color coded. Regions where the fluid flows faster are shown in red and correspond to high-speed streaks. Similarly, regions where the speed is lower are shown in blue and correspond to low-speed streaks.

vortices. An example of the coherent structures obtained is shown in **Figure 4**. All coherent states identified so far are, by construction, highly symmetric. They contain $n = 2, \ldots, 5$ vortex pairs that generate n or $2n$ high-speed streaks close to the wall and n low-speed streaks in the center. The high-speed streaks remain fairly rigid close to the walls, whereas the low-speed streaks wiggle considerably in the azimuthal direction. The vortex number does not fix the states uniquely: There can be several states with the same number of vortices (Wedin & Kerswell 2004).

The critical value for the appearence of the coherent states depends on their wavelength. The one with the lowest critical Reynolds number has three vortex pairs and appears in a saddle node bifurcation near $Re = 1250$ with an axial wavelength of 2.1 d. Actually, there are several similar states that appear at comparable Reynolds numbers (Wedin & Kerswell 2004). The state with two vortex pairs arises at about $Re = 1350$, and the one with four at $Re = 1690$. The critical Reynolds numbers continue to increase as more vortices are added.

Interestingly, only the states with two or more vortex pairs give rise to symmetric coherent traveling states. The one with a single pair, which gives the strongest linear amplification (Schmid & Henningson 1994, Zikanov 1996), does not. A less symmetric version of a two-vortex state appears in a different context in Section 5.

4.2. Detecting the Structures in Experimental Data

Turbulent dynamics has a positive Lyapunov exponent and is chaotic, so how can the coherent structures show up in experiments?

One can imagine that the orbit in state space will reside for some time in the vicinity of the unstable saddle points. Around each saddle point one can define a region for which the flow state is close enough to the saddle point so that the flow pattern is very similar to the traveling wave solution. Provided that the residence time within each of these volumes is at least a substantial fraction of the transit time from one coherent state to the next coherent state, it is possible to detect a flow pattern that has a strong resemblance to the exact traveling wave solutions. However, due to

the strongly unstable character of the traveling wave solutions, the correspondence will be more of a qualitative nature than an exact quantitative one. Furthermore, the ratio of residence time and transit time will (rapidly) decrease for increasing Reynolds number: (*a*) With increasing Reynolds number, the number of coherent flow states increases, which likely reduces the probability of finding the flow in the vicinity of any of the coherent states, and (*b*) it is likely that the volume for which the flow state is sufficiently close to the saddle point becomes smaller for increasing Reynolds number. Hence, one can only expect to find flow patterns that resemble those of the coherent flow states in the low Reynolds number region. Because the flow state is not likely identical to the exact traveling wave solutions, one must rely on the appearance of the main features, i.e., the azimuthal periodicity of the high-speed and low-speed regions, and the presence of the vortex rolls for its detection.

Empirically, one can then define an indicator for the coherent structures and study the frequency with which this indicator signals their presence (Hof, van Doorne et al. 2004; T.M. Schneider, J. Vollmer & B. Eckhardt, in preparation). Ideally, this indicator would check how well the spatial structures of all velocity components match, but in view of the many dimensions, an inaccessibly large number of experiments and realizations would be required. Experimentally and theoretically, the approach is to allow a projection onto a lower dimensional subspace and to consider the frequency of appearance in that subspace. Hof, van Doorne et al. (2004) use a correlation function that focuses on the prominent downstream vortices and their symmetry for the projection.

Projecting this correlation function onto frequencies of three and four vortex pairs, combined with a threshold, allows us to identify the presence of such coherent arrangements in several regions of the flow. This was first applied to experimental data in a long water-filled pipe flow facility obtained from a stereoscopic particle image velocimetry (PIV) system (Hof, van Doorne et al. 2004). The pipe in this facility has a 40-mm inner diameter with a total pipe length of 26 m. A carefully designed contraction and flow-conditioning section at the inlet allows the realization of laminar pipe flow over the full length of the pipe up to a Reynolds number of 60×10^3. The volume flow rate is maintained at a constant level by means of a feedback loop connecting the pump to an electromagnetic flow meter.

The PIV measurement technique yields all three instantaneous velocity components in a cross section of the flow perpendicular to the pipe axis. The velocity information is obtained from the motion of small particles carried by the flow, which are illuminated by means of a thin light sheet generated from a pulsed laser system and which are observed by two cameras in a stereoscopic configuration. This configuration makes it possible to determine the secondary flow patterns represented primarily in the radial and azimuthal velocity components, which are an order of magnitude smaller than the axial velocity component. Details of the experimental configuration and the validation of the measurement precision will be given by C.W.H. van Doorne & J. Westerweel (under revision).

The high sampling speed and the spatial resolution of the cameras made it possible to obtain good temporal and spatial resolution of the velocity fields up to Reynolds numbers of about 5000. By calculating the azimuthal correlation of the streamwise velocity, coherent flow states could be identified. The arrangements of the vortex

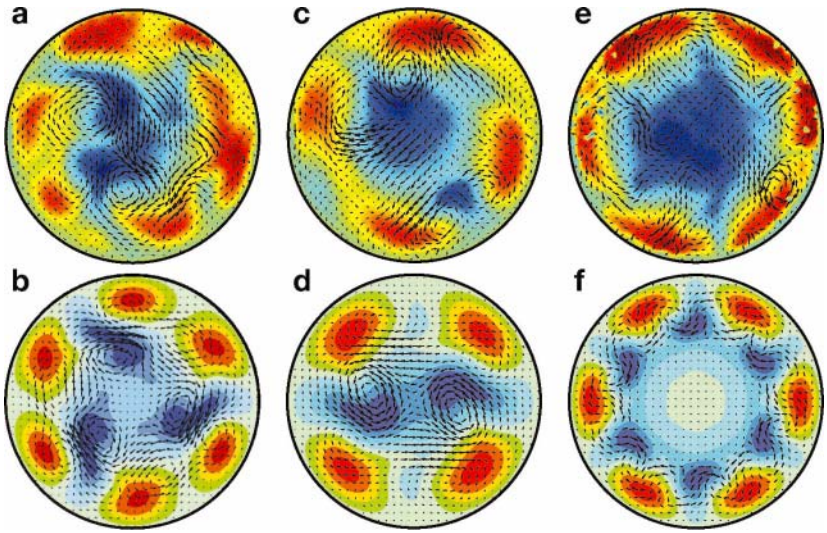

Figure 5

Pairing (*a* & *b*, *c* & *d*, *e* & *f*) between flow structures detected in experimental cross sections (*top row*) and numerically determined traveling waves (*bottom row*). The representation of the velocity fields is the same as in **Figure 4**. From Hof, van Doorne et al. (2004).

rolls and high- and low-speed streaks of these states closely resemble those of the traveling waves.

By means of this analysis several coherent flow states could be identified in both fully developed turbulent pipe flow and turbulent puffs traveling through the pipe (see **Figure 5**): Coherent flow states with three and two vortex pairs were observed in turbulent puffs at Re = 2000–2500, and coherent flow states with four and six vortex pairs were observed in fully developed turbulence at Re = 3000 and Re = 5300, respectively. As mentioned above, one cannot expect to find the exact traveling wave solutions due to the unstable nature, but the observed flow patterns would at least show the main features, such as the counter-rotating vortices and low-speed and high-speed flow regions. The observed patterns will be disturbed as they do not occur as isolated and carefully balanced solutions—as in the Direct Numerical Simulations (DNS)—but occur in a natural strongly dissipative flow state. Nonetheless, the resemblance between the numerically found flow states and those observed in experiments is striking.

The full 3D velocity field can be recovered from a time series of stereoscopic PIV measurements at a fixed location by assuming that the velocity field changes slowly while it is advected downstream with the mean flow velocity (Taylor's frozen flow assumption). This reconstruction makes it possible to determine the structure of the coherent states in the axial direction (Hof et al. 2005). In agreement with the observations for the exact traveling wave solutions, the low-speed streaks observed experimentally showed a clear wavy modulation in the streamwise direction. For several of these observations, the duration of the observed coherent flow state was sufficient to observe pairs of counter-rotating vortices along the streaks, and hence to obtain an estimate of the wavelength of the coherent flow state (see **Figure 6**). The length scale of the wavy modulation as well as the distance between vortex pairs observed was in good agreement with those found for the traveling wave solutions.

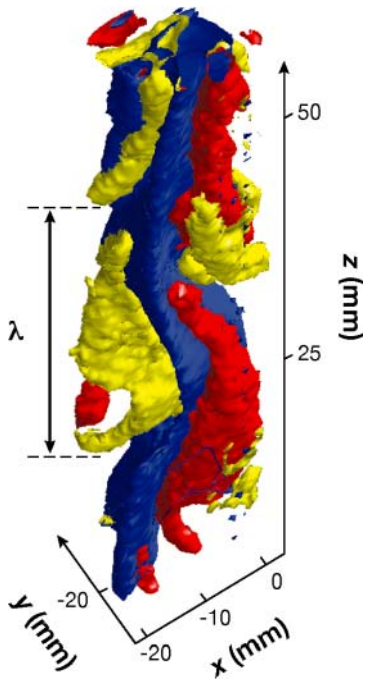

Figure 6

A section of a puff with the coherent structures and their wavelength highlighted. Positive and negative vorticity is shown in yellow and red. The wavy low-speed streak (shown in *blue*) is sandwiched between counter-rotating streamwise streaks, identified through the vorticity distribution. From Hof et al. (2005).

Hence, the most characteristic features of these traveling wave solutions, i.e., the counter-rotating vortices in conjunction with high-speed and low-speed streaks, as well as the wavelength for these coherent flow states, could be observed in the flow patterns of actual pipe flows. Further experiments are currently being evaluated to determine the relative occurence of these coherent flow states.

5. EDGE OF CHAOS

The coexistence of stable laminar and turbulent dynamics naturally leads to questions regarding the nature of the boundary between them. Scanning the dynamics for initial conditions, obtained, for example, by adding a perturbation of fixed spatial structure but varying amplitude to the laminar profile, one can distinguish regions with smooth variations in lifetime from regions with irregular variations (see the sketch in **Figure 7**). The points between the smooth and chaotic regions lie on the edge of chaos: Operationally, they can be detected as the first initial conditions with infinite lifetimes when coming from the laminar side. They stay away from the laminar profile, but they also do not swing up to the turbulent dynamics. Numerical

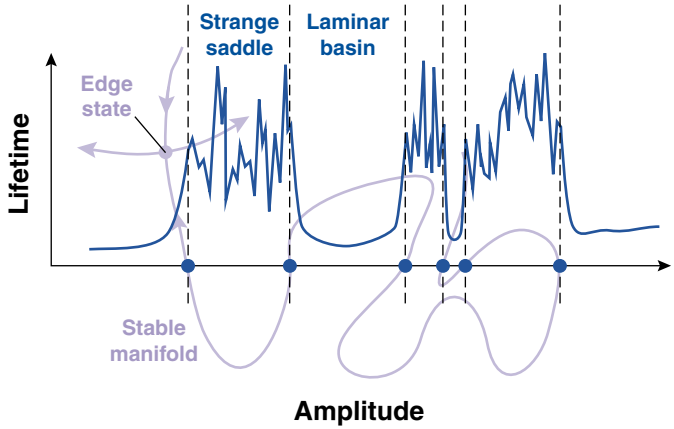

Figure 7

Edge of chaos in shear flows. By increasing the amplitude of a perturbation, one can distinguish regions with smooth variations in lifetimes and others with irregular variations (*dark blue line*). The limiting points between the two regions are on the edge of chaos. As indicated by the line connecting them (*lavender line*), they belong to the stable manifold of an invariant structure that separates the laminar from the turbulent. From Skufca et al. (2005).

simulations and theoretical considerations suggest that they collapse onto structures that are attracting within the edge of chaos, but are unstable perpendicular to it, so-called relative attractors. The relative attractors can be simple, such as traveling waves, but can also be fairly complicated chaotic objects.

The invariant structures in the edge of chaos can be obtained by direct shooting methods (as in Itano & Toh 2001) or by successive refinements that enable one to follow the edge of chaos for longer times (as in Skufca et al. 2005). For pipe flow we have tracked this intermediate state for lifetimes up to 2500 R/u_c. The edge state is dominated by a pair of vortices that are off center, and shows a persistent dynamic variation of the low-speed streaks in the center (see **Figure 8**).

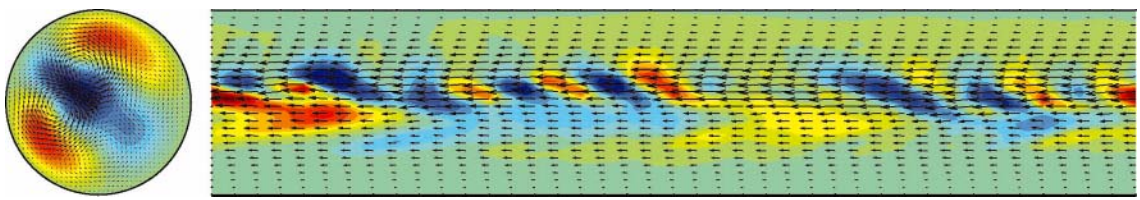

Figure 8

The structure of the edge state in a pipe flow at a Reynolds number of 2875. The cross section on the left is dominated by two off-center vortex pairs and their high-speed streaks close to the wall. The slice along the axis at an angle that cuts right through the middle of the two vortices shows the downstream variation. The absence of any periodicity is indicative of the persistent dynamics of the edge state.

6. SUMMARY

In the previous sections we emphasized the dynamical system characteristics of transition to turbulence in pipe flow, including the critical amplitude for transition, the sensitive dependence on initial conditions in the transition region, the lifetime distribution, and the edge of chaos. In this section we summarize these findings and put them into perspective under three different headings: critical Reynolds number, coherent structures, and transition mechanism.

6.1. Critical Reynolds Numbers

The intermittent dynamics in the transition region implies that values of critical Reynolds numbers depend on the specific definition. For pipe flow one can distinguish the following four situations:

The strongest requirement for the evolution of a perturbation to a flow is that its energy content decays monotonically for any initial condition: This is the requirement of energy stability. The associated critical Reynolds number Re_E can be determined from an analysis of the linearized equations of motion. For pipe flow this gives $R_E = 81.5$ (Joseph 1976).

Next, one can give up monotonicity, but still require that any perturbation decays eventually. This defines the critical Reynolds number Re_G for global stability. A system is globally stable if the laminar profile is the only permanently sustained state in the system. The Reynolds numbers Re_{TW_i}, at which any stationary state or traveling wave appears, provide upper bounds on Re_G, i.e., $Re_G = \min Re_{TW_i}$. From the coherent structures described in Faisst & Eckhardt (2003) and Wedin & Kerswell (2004), one concludes that $R_G \leq 1250$. Although we expect this to be the lowest value within the class of traveling waves studied, it cannot be ruled out that other structures, perhaps with less symmetry or more complicated time dependence, already occur at even lower Reynolds numbers.

Experimentally, a transition to turbulence is not observed until somewhat larger values. To eliminate the influence of the sensitive dependence on initial conditions, in Section 3 we advocate the use of probabilities. The probability $P(t, Re)$ to remain turbulent for at least a time t at a Reynolds number Re shows an exponential tail that is free from the details of the initial perturbation and can be characterized by a well-defined time. From this distribution one can extract a critical Reynolds number $Re_{\rm exp}$, for instance, by requiring that over the duration of the experiment ($t_{\rm exp}$) only 10% of all repetitions decay: determine $Re_{\rm exp}$ such that $P(t_{\rm exp}, Re_{\rm exp}) = 0.9$. The rapid increase in lifetimes suggests that even for the longest pipes such a value will remain below about 2250 (this is the value from DNS as it is the largest value reported so far; experiments point to a lower value, as discussed in Section 3).

Finally, the decreasing critical amplitude needed to trigger turbulence suggests that for sufficiently high Reynolds numbers it is impossible to maintain the laminar profile. Effects like thermal fluctuations, compressibility, and deviations in the profile due to Coriolis forces, alignment of the tube, or smoothness of the surface will become important. The mathematical version of these problems is rooted in the

non-normality of the linearized problem. As Meseguer & Trefethen (2003) describe, at Reynolds numbers $Re \sim 10^5$ perturbations as small as 10^{-5} can suffice to introduce growing eigenmodes. The Reynolds number where such tiny perturbations begin to dominate is not universal, but finite.

6.2. Coherent Structures

A great deal of effort has focused on detecting and characterizing coherent structures in turbulent flows (see, for instance, Holmes et al. 1996, Panton 2001, Robinson 1991). The traveling waves provide a dynamical and fully nonlinear approach to the problem. Traveling waves share with the usual coherent structures the presence of some large-scale features, a predictable dynamics, and a relatively frequent occurence. They have the additional bonus of being exact solutions to the equations of motion, which is why the term "exact coherent structures" has been suggested (Waleffe 1998, 2001, 2003). A link between coherent structures and dynamical systems was also proposed by Itano & Toh (2001) and Toh & Itano (2005).

The possibility of connecting coherent states to specific exact dynamical solutions to the equations of motion and to certain regions of the state space of the flow is an intriguing one, and only partially explored thus far. Ideally, one would like to be able to identify coherent features and calculate their relative frequency from the equations of motion. Quantitative studies of their statistical properties, like frequency, persistence, or contribution to momentum transport, and an accurate description of the dynamics near the states should open up new ways to influence flows and to predict the effects of flow control.

6.3. Transition Mechanism

Experimental studies have long shown that certain flow patterns (hairpins, etc.) appear and grow during transition to turbulence. The dynamical system picture for the edge of chaos (see **Figure 7**) suggests that these features should be connected with the invariant state in the edge of chaos (see Itano & Toh 2001, Skufca et al. 2005). Certainly, the presence of two strong vortices connects the results from non-normal amplification, which show that this structure gives the strongest amplification (Schmid & Henningson 1994, Zikanov 1996). The edge of chaos analysis in Skufca et al. (2005) suggests techniques that can be used quite generally to trace the dynamics at the border between laminar and turbulent flows, and hence to determine the relevant flow patterns and features. Itano & Toh (2001) link the appearance of bursts to the escape from the edge state along the unstable manifold. These studies provide a framework for further investigations of the intermittent dynamics in the equilibrium turbulent state. It is particularly intriguing that the theory suggests that, except for symmetries, there is one and only one invariant object, which together with its stable manifold separates the laminar from the turbulent region. The characteristics of this state are a pair of vortices off center, closer to the walls. Interestingly, a similar pair of vortices seems to be the edge state in plane Poiseuille flow, as reported by Itano & Toh (2001).

7. OUTLOOK

The methods described here carry over to several other shear flows where transition to turbulence occurs without linear instability of the laminar profile. Extensive numerical and experimental studies have identified the same scenario as described here for plane Couette flow (Bottin & Chaté 1998; Bottin et al. 1998; Clever & Busse 1992, 1997; Dauchot & Daviaud 1994, 1995; Daviaud et al. 1992; Eckhardt et al. 2002; Faisst & Eckhardt 2000; Nagata 1990; Schmiegel & Eckhardt 1997; Waleffe 1995, 1998, 2001, 2003). Plane Poiseuille flow is peculiar as it has a linear instability, albeit at Reynolds numbers of about 5772—well above the values where transition is first observed. However, coherent states and traveling waves have been identified there as well (Ehrenstein & Koch 1991, Itano & Toh 2001, Waleffe 2003). Undoubtedly, similar phenomenology can be expected in external boundary layers.

The identification of traveling waves and the possibility that chaos is organized around them suggest that it might be possible to treat the statistical properties of the flow in terms of such coherent states. In low-dimensional dynamical systems this goes under the heading of periodic orbit theory, where one can show that by exploiting a symbolic ordering of orbits one can efficiently and accurately calculate statistical properties (Artuso et al. 1990a,b; Christiansen et al. 1997; Cvitanovic & Eckhardt 1991; Ott & Eckhardt 1994). Some periodic solutions for plane Couette flow have already been found (Kawahara & Kida 2001, Toh & Itano 2003). Nevertheless, carrying this program through for turbulent flows, even in the transition region, remains a challenge. But the possibility of identifying certain coherent structures in numerical and experimental data suggests that even if the full program cannot be realized, some approximate realizations might be feasible and useful.

The main open question not addressed here is the relation between the periodic structures in the numerical simulations and the localized puffs and slugs in the unbounded domain. Structured turbulence, i.e., localized turbulent patches in boundary layers (Gad el Hak & Hussain 1986, Schumacher & Eckhardt 2001), turbulent sections in pipe flow (Wygnanski & Champagne 1973, Wygnanski et al. 1975), or banded turbulence in plane Couette and Taylor-Couette flow (Barkley & Tuckerman 2005, Prigent et al. 2002), has been documented repeatedly, but the mechanisms remain to be elucidated. Because the turbulent patches are much larger than the typical wavelengths of the coherent structures studied here, one might hope that the puff-and-slug-forming process is a long-wavelength dynamics on top of the coherent structures described here.

ACKNOWLEDGMENTS

B.E. would like to thank the members of the Burgers Board at the University of Maryland, in particular Dan Lathrop, for their hospitality during 2004–2005. We thank G. Homsy and K.S. Breuer for permission to include the movies of Reynolds's experiment with the online material. We also thank the Deutsche Forschungsgemeinschaft and the Foundation for Fundamental Research on Matter for support.

LITERATURE CITED

Aref H, Kadtke JB, Zawadzki I, Campbell LJ, Eckhardt B. 1988. Point vortex dynamics: recent results and open problems. *Fluid Dyn. Res.* 3:63–74

Aref H. 1983. Integrable, chaotic, and turbulent vortex motion in two-dimensional flows. *Annu. Rev. Fluid Mech.* 15:345–89

Artuso R, Aurell E, Cvitanovic P. 1990a. Recycling of strange sets: I. Cycle expansions. *Nonlinearity* 3:325–59

Artuso R, Aurell E, Cvitanovic P. 1990b. Recycling of strange sets: II. Applications. *Nonlinearity* 3:361–86

Barkley D, Tuckerman LS. 2005. Computational study of turbulent laminar patterns in Couette flow. *Phys. Rev. Lett.* 94:014502

Boberg L, Brosa U. 1988. Onset of turbulence in a pipe. *Z. Naturforsch.* 43a:697–726

Bottin S, Daviaud F, Manneville P, Dauchot O. 1998. Discontinuous transition to spatiotemporal intermittency in plane Couette flow. *Europhys. Lett.* 43(2):171–76

Bottin S, Chaté H. 1998. Statistical analysis of the transition to turbulence in plane Couette flow. *Eur. Phys. J. B.* 6:143–55

Brosa U. 1989. Turbulence without strange attractor. *J. Stat. Phys.* 55:1303–12

Chapman SJ. 2002. Subcritical transition in channel flows. *J. Fluid. Mech.* 451:35–97

Cherhabili A, Ehrenstein U. 1997. Finite-amplitude equilibrium states in plane Couette flow. *J. Fluid Mech.* 342:159–77

Christiansen F, Cvitanovic P, Putkaradze V. 1997. Spatiotemporal chaos in terms of unstable recurrent patterns. *Nonlinearity* 10:55–70

Clever RM, Busse FH. 1992. Three-dimensional convection in a horizontal fluid layer subjected to a constant shear. *J. Fluid Mech.* 234:511–27

Clever RM, Busse FH. 1997. Tertiary and quaternary solutions for plane Couette flow. *J. Fluid Mech.* 344:137–53

Crutchfield JP, Kaneko K. 1988. Are attractors relevant to turbulence? *Phys. Rev. Lett.* 60:2715–18

Cvitanovic P, Eckhardt B. 1991. Periodic orbit expansion for classical smooth flows. *J. Phys. A.* 24:L237–41

Darbyshire AG, Mullin T. 1995. Transition to turbulence in constant-mass-flux pipe flow. *J. Fluid Mech.* 289:83–114

Dauchot O, Daviaud F. 1994. Finite amplitude perturbation in plane Couette flow. *Europhys. Lett.* 28:225–30

Dauchot O, Daviaud F. 1995. Finite amplitude perturbation and spot growths mechanism in plane Couette flow. *Phys. Fluids* 7:335–43

Daviaud F, Hegseth J, Bergé P. 1992. Subcritical transition to turbulence in plane Couette flow. *Phys. Rev. Lett.* 69:2511–14

Doering CR, Gibbon JD. 1995. *Applied Analysis of the Navier-Stokes Equation*. Cambridge, UK: Cambridge Univ. Press

Draad AA, Kuiken GDC, Nieuwstadt FTM. 1998. Laminar-turbulent transition in pipe flow for Newtonian and non-Newtonian fluids. *J. Fluid Mech.* 377:267–312

Eckhardt B, Yao D. 1993. Local Lyapunov exponents. *Physica. D.* 65:100–8

Eckhardt B, Aref H. 1988. Integrable and chaotic motions of four vortices: II. Collision dynamics of vortex pairs. *Phil. Trans. R. Soc. London A* 326:655–96

Eckhardt B, Faisst H. 2004. Dynamical systems and the transition to turbulence. In *Laminar-Turbulent Transition and Finite Amplitude Solutions*, ed. T Mullin, RR Kerswell, pp. 35–50. Dordrecht: Springer

Eckhardt B, Faisst H, Schmiegel A, Schumacher J. 2002. Turbulence transition in shear flows. In *Advances in Turbulence IX*, eds. I Castro, P Hanock, T Thomas. pp. 701–8. Barcelona: CISME

Ehrenstein U, Koch W. 1991. Three-dimensional wavelike equilibrium states in plane Poiseuille flow. *J. Fluid. Mech*. 228:111–48

Faisst H, Eckhardt B. 2000. Transition from the Couette-Taylor system to the plane Couette system. *Phys. Rev. E*. 61:7227–30

Faisst H, Eckhardt B. 2003. Traveling waves in pipe flow. *Phys. Rev. Lett*. 91:224502

Faisst H, Eckhardt B. 2004. Sensitive dependence on initial conditions in transition to turbulence in pipe flow. *J. Fluid Mech*. 504:343–52

Gad-el-Hak M, Hussain AKMF. 1986. Coherent structures in a turbulent boundary layer. *Phys. Fluids* 29:2124–39

Grebogi C, Ott E, Yorke JA. 1982. Chaotic attractors in crisis. *Phys. Rev. Lett*. 48:1507–10

Grossmann S. 2000. The onset of shear flow turbulence. *Rev. Mod. Phys*. 72:603–18

Guckenheimer J. 1986. Strange attractors in fluids: another view. *Annu. Rev. Fluid Mech*. *18*:15–31

Guckenheimer J, Holmes P. 1983. *Nonlinear Oscillations, Dynamical Systems, and Bifurcations of Vector Fields*. New York: Springer-Verlag

Hagen G. 1839. Über die Bewegung des Wassers in engen zylindrischen Röhren. *Pogg. Ann*. 46:423

Hagen G. 1854. Über den Einfluß der Temperatur auf die Bewegung des Wassers in Röhren. *Abh. Akad. Wiss. Ber.* pp. 17–98

Hamilton JM, Kim J, Waleffe F. 1995. Regeneration mechanisms of near-wall turbulence structures. *J. Fluid Mech*. 287:317–48

Henningson DS. 1996. Comment on "Transition in shear flows. Nonlinear normality versus non-normal linearity". *Phys. Fluids* 8:2257–58

Hof B. 2004. Transition to turbulence in pipe flow. In *Laminar-Turbulent Transition and Finite Amplitude Solutions*, ed. T Mullin, RR Kerswell, pp. 221–31. Dordrecht: Springer

Hof B, Juel A, Mullin T. 2003. Scaling of the turbulence transition threshold in a pipe. *Phys. Rev. Lett*. 91:244502

Hof B, van Doorne CWH, Westerweel J, Nieuwstadt FTM. 2005. Turbulence regeneration in pipe flow at moderate Reynolds numbers. *Phys. Rev. Lett*. 95:214502

Hof B, van Doorne CWH, Westerweel J, Nieuwstadt FTM, Faisst H, et al. 2004. Experimental observation of nonlinear traveling waves in turbulent pipe flow. *Science* 305:1594–98

Hof B, Westerweel J, Schneider TM, Eckhardt B. 2006. Finite lifetime of turbulence in shear flows. *Nature* 443:59–62

Holmes P, Lumley JL, Berkooz G. 1996. *Turbulence, Coherent Structures, Dynamical Systems, and Symmetry*. Cambridge, UK: Cambridge Univ. Press

Homsy GM, Aref H, Breuer KS, Hochgreb S, Koseff JR, et al. 2004. *Multimedia Fluid Mechanics*. Cambridge, UK: Cambridge Univ. Press

Itano T, Toh S. 2001. The dynamics of bursting process in wall turbulence. *J. Phys. Soc. Japan* 70:703–16
Joseph DD. 1976. *Stability of Fluid Motions, Vol. I and II.* Berlin: Springer
Kadanoff LP, Tang C. 1984. Escape from strange repellers. *Proc. Natl. Acad. Sci. USA* 81:1276
Kaneda K. 1990. Supertransients, spatiotemporal intermittency and stability of fully developed spatiotemporal chaos. *Phys. Lett. A*. 149:105–12
Kawahara G, Kida S. 2001. Periodic motion embedded in plane Couette turbulence: regeneration cycle and burst. *J. Fluid Mech*. 449:291–300
Kerswell RR. 2005. Recent progress in understanding the transition to turbulence in a pipe. *Nonlinearity* 18:R17–44
Lanford OE III. 1982. The strange attractor theory of turbulence. *Annu. Rev. Fluid Mech*. 14:347–64
Meseguer A, Trefethen LN. 2003. Linearized pipe flow at Reynolds numbers 10,000,000. *J. Comp. Phys*. 186:178–97
Moehlis J, Faisst H, Eckhardt B. 2004. A low-dimensional model for turbulent shear flows. *New J. Phys.* 6:Art. 56
Mullin T, Peixinho J. 2006. Recent observations in the transition to turbulence in a pipe. In *IUTAM Symposium on Laminar-Turbulent Transition*, ed. R Govindarajan. p. 45. Bangalore: Springer
Mullin T, Kerswell R. 2005. *IUTAM Symposium on Laminar-Turbulent Transition and Finite Amplitude Solutions*. Dordrecht: Springer
Nagata M. 1990. Three-dimensional finite-amplitude solutions in plane Couette flow: bifurcation from infinity. *J. Fluid Mech*. 217:519–27
Ott E. 1993. *Chaos in Dynamical Systems*. Cambridge, UK: Cambridge Univ. Press
Ott G, Eckhardt B. 1994. Periodic orbit analysis of the Lorenz attractor. *Z. Phys. B* 94:259–66
Panton RL. 2001. Overview of the self-sustaining mechanisms of wall turbulence. *Prog. Aerospace. Sci*. 37:341–83
Peixinho J, Mullin T. 2006. Decay of turbulence in pipe flow. *Phys. Rev. Lett*. 96:094501
Poiseuille JLM. 1840. Recherches expérimentelles sur le mouvement des liquides dans les tubes de trés petits diamètres. *Comp. Rend*. 11:961–67, 1041–48
Prigent A, Gregoire G, Chate H, Dauchot O, van Saarloos W. 2002. Large-scale finite-wavelength modulation within turbulent shear flows. *Phys. Rev. Lett*. 89:014501
Reynolds O. 1883. An experimental investigation of the circumstances which determine whether the motion of water shall be direct or sinuous and the law of resistance in parallel channels. *Phil. Trans. R. Soc*. 174:935–82
Robinson SK. 1991. Coherent motions in the turbulent boundary layer. *Annu. Rev. Fluid Mech*. 23:601–39
Salwen H, Cotton FW, Grosch CE. 1980. Linear stability of Poiseuille flow in a circular pipe. *J. Fluid Mech*. 98:273–84
Schmid PJ, Henningson DS. 1994. Optimal energy growth in Hagen-Poiseuille flow. *J. Fluid Mech*. 277:197

Schmid PJ, Henningson DS. 1999. *Stability and Transition of Shear Flows*. New York: Springer
Schmiegel A, Eckhardt B. 1997. Fractal stability border in plane Couette flow. *Phys. Rev. Lett*. 79:5250–53
Schumacher J, Eckhardt B. 2001. Evolution of turbulent spots in a parallel shear flow. *Phys. Rev. E*. 63:046307
Skufca J, Yorke JA, Eckhardt B. 2006. The edge of chaos in a model for a parallel shear flow. *Phys. Rev. Lett*. 96:174101
Toh S, Itano T. 2003. A periodic-like solution in channel flow. *J. Fluid Mech*. 481:67–76
Toh S, Itano T. 2005. Interaction between a large-scale structure and near-wall structures in channel flow. *J. Fluid Mech*. 524:249–62
Trefethen LN, Trefethen AE, Reddy SC, Driscoll TA. 1993. Hydrodynamic stability without eigenvalues. *Science* 261:578–84
Waleffe F. 1995. Transition in shear flows: non-linear normality versus non-normal linearity. *Phys. Fluids* 7:3060–66
Waleffe F. 1998. Three-dimensional coherent states in plane shear flows. *Phys. Rev. Lett*. 81(19):4140–43
Waleffe F. 2001. Exact coherent structures in channel flow. *J. Fluid Mech*. 435:93–102
Waleffe F. 2003. Homotopy of exact coherent structures in plane shear flows. *Phys. Fluids* 15:1517–34
Wedin H, Kerswell RR. 2004. Exact coherent structures in pipe flow: traveling wave solutions. *J. Fluid Mech*. 508:333–71
Wygnanski IJ, Champagne FH. 1973. On transition in a pipe. Part 1. The origin of puffs and slugs and the flow in a turbulent slug. *J. Fluid Mech*. 59:281–335
Wygnanski IJ, Sokolov M, Friedman D. 1975. On transition in a pipe. Part 2. The equilibrium puff. *J. Fluid Mech*. 69:283–304
Zikanov OY. 1996. On the instability of pipe Poiseuille flow. *Phys. Fluids* 8(11):2923–32

Annual Review of
Fluid Mechanics

Volume 39, 2007

Contents

Indexes

Errata

An online log of corrections to *Annual Review of Fluid Mechanics* chapters (1997 to the present) may be found at http://fluid.annualreviews.org/errata.shtml